  Bull. Chem. Soc. Jpn., 53, 3093—3099 (1980)

Thermal Decomposition of Graphite Fluoride. II. Kinetics of Thermal Decomposition of $(CF)_n$ in a Vacuum

Nobuatsu WATANABE* and Satoshi KOYAMA

Department of Industrial Chemistry, Faculty of Engineering, Kyoto University, Yoshida, Sakyo-ku, Kyoto 606

(Received April 3, 1980)

The rate of thermal decomposition of $(CF)_n$ prepared under several reaction conditions was measured in a vacuum. The rate was expressed by Avrami-Erofeyev's equation of second-order for highly oriented sample and of first-order for disordered one. The apparent activation energies of the decomposition reaction were about 50 kcal/mol (1 cal=4.184 J) for the former, and about 14 kcal/mol in higher temperature region and about 100 kcal/mol in lower temperature region for the latter. Thermal decomposition of $(CF)_n$ proceeds two-dimensionally around a nucleus of carbon which is formed at the initial stage of decomposition. The rate of thermal decomposition of various samples is dependent on the number of the nucleus forming sites. The nucleation of carbon takes place on a grain boundary between two small crystallites of $(CF)_n$. The rate of the growth of the nucleus is fast along the grain boundary but slow in other directions. The activation energy was estimated to be about 100 kcal/mol for the former and almost 0 kcal/mol for the latter.

It is well-established that the physicochemical properties of graphite fluoride depend both on those of original carbon materials and fluorination conditions.[1,2] DTA studies revealed that decomposition temperature of $(CF)_n$ samples varied widely between 320 and 610 °C. Detailed analyses of the decomposition products of $(CF)_n$ in a vacuum have also been made, and it was found that thermal decomposition can be expressed by the following equation,[3]

$$2(CF)_n \longrightarrow nC^* + XCF_2 + YC_2F_4, \quad (1)$$

where $X+2Y=n$ and C* is amorphous carbon. Then, these gaseous products give various compounds such as CF_4, C_2F_6, C_3F_8, *etc.*

Recently this reaction was also studied by Kamarchik and Margrave.[4] They have used Avrami-Erofeyev's equation to analyze their kinetic data.

$$-\ln(1-\alpha) = (kt)^n, \quad (2)$$

where α is the fraction decomposed, k is the rate constant, and n is the dimension of the nucleus growth. The value of n was found to be 2. This result suggests that the decomposition proceeds two-dimensionally around an active site or a nucleus, and the reaction is of an auto-catalytic type. However, they could not make clear the reason why the rate of thermal decomposition of $(CF)_n$ samples varied with their formation conditions.

In this work, thermal decomposition of $(CF)_n$ prepared from various carbon materials was investigated in more detail. Based on the kinetic studies, we will discuss how the reaction (Eq. 1) proceeds in a particle or crystal of $(CF)_n$, and why the thermal behavior of samples differs from each other. In addition, microscopic observation has been made with $(CF)_n$ before and after the decomposition, and we also discuss where the decomposition begins, and how the nucleus grows.

Experimental

Preparation and Some Properties of $(CF)_n$ Samples. The samples used for the measurement of decomposition rate were prepared from (I) flaky natural graphite whose grain size was 279—840 μm, (II) powdery natural graphite whose grain size was 46—62 μm, and (III) petroleum coke (<37 μm).

The samples I and II were prepared by using a rotary reactor for fluorination.[5] Table 1 shows some properties and formation conditions of these samples. Crystallinity was measured by means of X-ray diffractometry. The crystallinity of the samples increases in the order of I>II>III. While the fluorine/carbon atomic ratio (F/C) of sample III is the highest. This is due to the presence of CF_2 or CF_3 groups on the particle surface of this $(CF)_n$ sample.[6]

In addition to the samples described in Table 1, another $(CF)_n$ sample has been prepared for microscopic observation in the following manner. A grain of flaky natural graphite of 2 mm in diameter was directly fluorinated in a thermo-balance type apparatus at 610 °C, for 48 h. Fluorine pressure was 26.6 kPa. The sample of $(CF)_n$ thus prepared was of flaky type. The size was about 2 mm in diameter (a and b axes) and about 0.5 mm in thickness (c axis), respectively.

Measurement of the Decomposition Rate and Microscopic Observation. A thermo-balance was used to measure the weight loss *vs.* time curve. The apparatus has been described in detail previously.[7] About 30 mg of $(CF)_n$ sample on a nickel boat was placed in the reaction tube of the apparatus. A pressure of 0.13 Pa was kept throughout the decomposition.

TABLE 1. PREPARATION CONDITION AND SOME PROPERTIES OF GRAPHITE FLUORIDE SAMPLE

Sample	Starting materials	Preparation condition		Crystallinity		F/C ratio	Color
		Temp/°C	t/h	d_{001}/Å	β_{001}/°		
I	Natural graphite (279—840 μm)	600	24	5.84	1.4	0.93	White
II	Natural graphite (46—62 μm)	600	11	6.00	2.5	0.94	Gray
III	Petroleum coke	420	Several	6.64	3.1	1.14	White

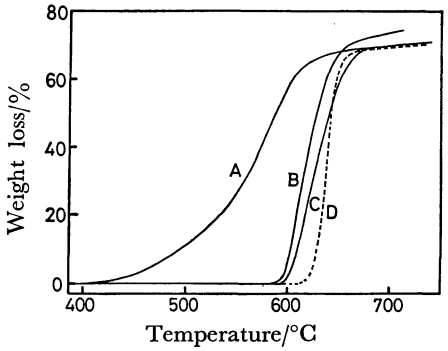

Fig. 1. TG curves for thermal decomposition of graphite fluoride in a vacuum.
A: Sample III, B: sample II, C: sample from natural graphite of 62—74 μm, D: sample I. Heating rate: 5 °C/min.

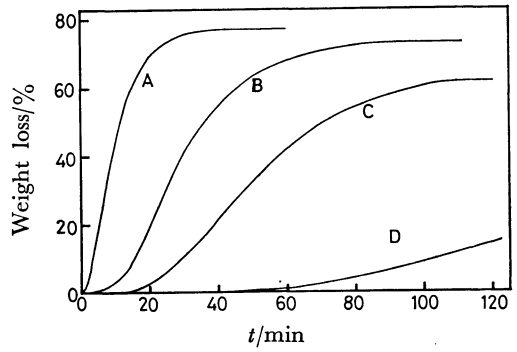

Fig. 2. Thermal decomposition of graphite fluoride (sample I) in a vacuum.
A: 668 °C, B: 654 °C, C: 616 °C, D: 599 °C.

The sample for microscopic observation was cleaved vertically along c axis. To do this, two fine rods of steel were sticked on both basal planes of a particle, then they were pulled off. These procedures were continued until the sample became sufficiently transparent. The sample thus formed was about 0.05 mm in thickness. The microscopic observation was carried out through this thin flake by means of either transmitted or reflected light, and in some cases, polarized light was used. The distribution of fluorine and carbon atoms in $(CF)_n$ sample was determined by X-ray microanalyzer.

Results and Discussion

Figure 1 shows TG curves for the decomposition of $(CF)_n$ sample given in Table 1 and of a sample from natural graphite of 62—74 μm. The heating rate was 5 °C/min. The decomposition of sample III which has a low crystallinity begins at lower temperature. However, the decomposition ended at the same temperature for all the samples, and their final weight loss was also constant value of about 70%. In the following discussion, the fraction decomposed, α is defined by $\alpha=w/w_f$, where w is the weight loss and w_f is the final weight loss. Since the final weight loss was 70%, α was given by $\alpha=w/0.7$.

Decomposition Rate of Samples I and II. Figure 2 shows the weight loss *vs.* time curves for the decomposition of sample I. Each curve has induction period,

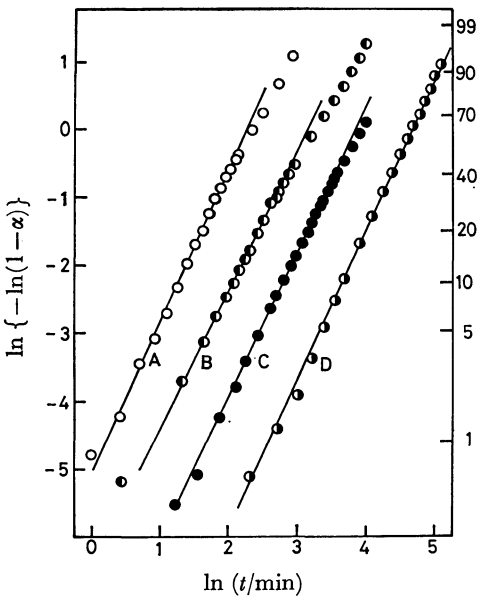

Fig. 3. $\ln\{-\ln(1-\alpha)\}$ *vs.* $\ln t$ plots for thermal decomposition of graphite fluoride (sample I).
A: 668 °C (n=2.24), B: 654 °C (n=2.05), C: 616 °C (n=2.12), D: 599 °C (n=2.18).

followed by acceleratory period and deceleratory period, that is, the curves are of sigmoid type. These curves are characteristic of the thermal decomposition of solids such as magnesite,[8] barium azide,[9] and other ionic crystals. The presence of induction and acceleratory periods shows that the reaction proceeds heterogeneously,[10] namely, a nucleus of the decomposition product is formed at a specific point in the crystal and spreads around the point.[11] In heterogeneous reactions, it is known that the rate equation for the decomposition of various kinds of compound is expressed by

$$\alpha = \frac{\sigma N_0}{V_0}(k_1 t)^n, \tag{3}$$

or

$$-\ln(1-\alpha) = \frac{\sigma N_0}{V_0}(k_1 t)^n, \tag{4}$$

where α is the fraction decomposed, σ is the shape factor of a nucleus, N_0 is the number of nucleus forming sites, V_0 is the final volume of the reaction products, k_1 is the linear rate constant of the growth of the nucleus and n is the dimension of the growth of nucleus. The curves shown in Fig. 2 could be expressed by Eq. 3 only for the region that the weight loss is less than 20%. However, the n value was varied from 1.5 to 2.1. This is because the overlapping of nuclei is not taken into account, and it becomes difficult to neglect the effect of overlapping as the nucleus grows. Equation 4 was derived by Avrami considering this effect.[12]

Then Eq. 4 was applied to the decomposition of $(CF)_n$, and $\ln\{-\ln(1-\alpha)\}$ was plotted against $\ln t$ in Fig. 3, in order to obtaine the n value. The plot gives a straight line for the region that α is less than 40% for samples I and II. For sample I, values in the range from 2.05 to 2.24 were obtained from the

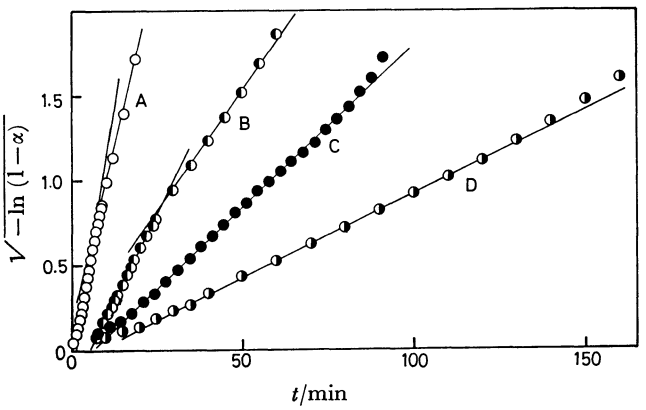

Fig. 4. $\sqrt{-\ln(1-\alpha)}$ *vs.* time plots for thermal decomposition of graphite fluoride (sample I) in a vacuum. A: 668 °C, B: 654 °C, C: 616 °C, D: 599 °C.

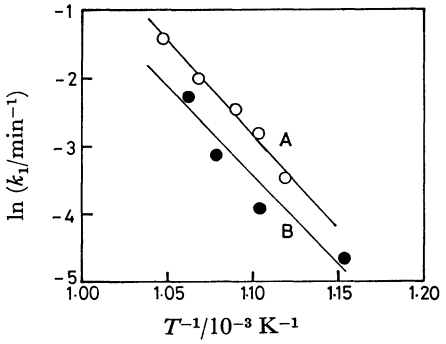

Fig. 5. The Arrhenius plots for decomposition of graphite fluoride.
A: Sample II, B: sample I. According to Eq. 3 (n=2).

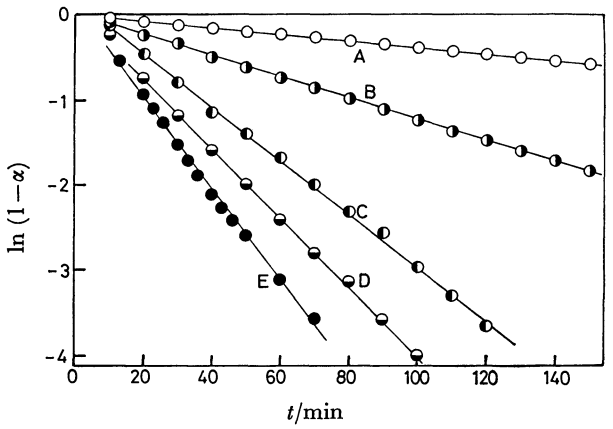

Fig. 6. $\ln(1-\alpha)$ *vs.* time plots for thermal decomposition of graphite fluoride (sample III) in a vacuum. A: 438 °C, B: 458 °C, C: 504 °C, D: 522 °C, E: 543 °C.

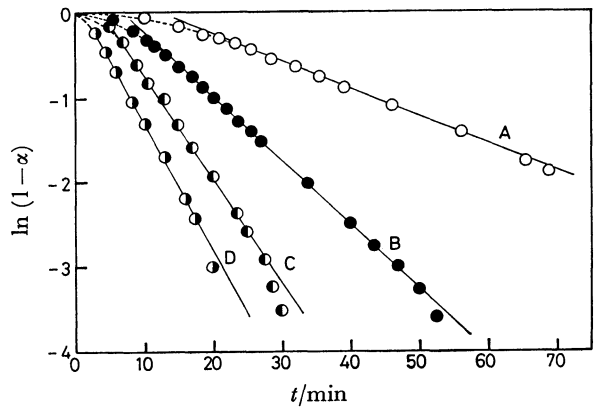

Fig. 7. $\ln(1-\alpha)$ *vs.* time plots for thermal decomposition of graphite fluoride (sample II) in a vacuum. A: 621 °C, B: 633 °C, C: 644 °C, D: 663 °C.

slopes of these plots as the dimension of the nucleus growth. This result suggests that the rate of the nucleation is sufficiently fast and that the dimension of the growth of nucleus is 2. Then $\sqrt{-\ln(1-\alpha)}$ was plotted against time in order to obtain the apparent rate constant in Fig. 4. This plot gives a straight line in the range of α=0—40% for sample I. The same plot for sample II also gives a straight line in the same range and the rate constant can be obtained from the slope. Figure 5 shows the Arrhenius plots for these two samples. The activation energy was 52.8 kcal/mol for sample II and 49.7 kcal/mol for sample I. The intercept to the ordinate $1/T$=0 was 26.8 and 24.0 for sample II and I, respectively. These values are given by $\ln A\sqrt{\sigma N_0/V_0}$, where A is the frequency factor of k_1. Since A, σ, and V_0 can be regarded as constant for these samples, the difference in the intercepts and the apparent reaction rate between the samples are due to the difference in N_0. It was found from the value of 26.8 and 24.0 that the number of nucleus forming site in sample II was about 300 times that in sample I.

It was found that the dimension of the nucleus growth is two and that the number of nucleus forming sites is different in each sample. These results suggest that the decomposition is initiated at CF_2 and CF_3 groups on the surface of $(CF)_n$ crystal or at a point on the region which is highly strained as reported on the decomposition by γ-ray[13] and by heat.[14] They also suggest that the nuclei formed spread two-dimensionally in parallel with the layer plane.

Decomposition Rate of Samples II and III. In contrast to the samples I and II, smaple III is a fine powdery sample prepared from petroleum coke. The weight loss *vs.* time curve for this sample has almost no acceleratory period and exhibits deceleratory curve from the beginning since the overlapping will take place as soon as the decomposition starts. The reaction rate is then expressed by the first-order equation:

$$-\ln(1-\alpha) = kt, \tag{5}$$

where k is the apparent rate constant. Figure 6 shows $\ln(1-\alpha)$ *vs.* time plots for this sample. The same plots for sample II also gave straight lines in the region where the weight loss is more than 20% (see Fig. 7). The Arrhenius plots for sample III at 480 °C or above can be approximated by a straight line (see Fig. 8), and the activation energy was calculated to be about 14 kcal/mol. On the other hand, it was about 100 kcal/mol below this temperature. This fact suggests that the rate-determining step at higher temperatures differs from that at lower tem-

TABLE 2. RATE EQUATION FOR THERMAL DECOMPOSITION OF GRAPHITE FLUORIDE IN A VACUUM

Sample	% decomposed					
	0—30%		30—40%		40—100%	
	Equation	E_a/kcal/mol	Equation	E_a/kcal/mol	Equation	E_a/kcal/mol
I	$\alpha=(kt)^2$					
	$\ln(1-\alpha)=-(kt)^2$	49.7	$\ln(1-\alpha)=-(kt)^2$	49.7		
II	$\alpha=(kt)^2$		$\ln(1-\alpha)=-kt$	100	$\ln(1-\alpha)=-kt$	100
	$\ln(1-\alpha)=-(kt)^2$	52.8	$\ln(1-\alpha)=-(kt)^2$	52.8		
III	$\alpha=(kt)^2$					
	$\ln(1-\alpha)=-kt$	14.4[a] 100[b]	$\ln(1-\alpha)=-kt$	14.4[a] 100[b]	$\ln(1-\alpha)=-kt$	14.4[a] 100[b]

a) Above 480 °C. b) Below 480 °C.

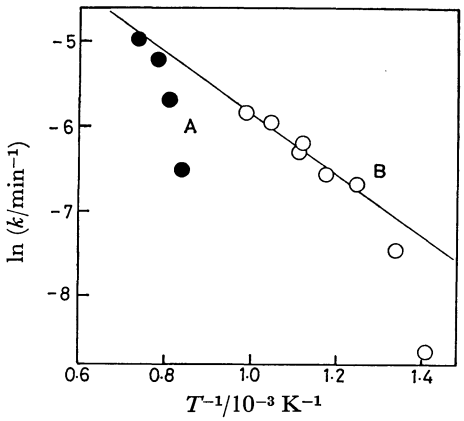

Fig. 8. The Arrhenius plots for decomposition of graphite fluoride.
A: Sample II, B: sample III. According to Eq. 5.

peratures. For sample II the activation energy was calculated to be about 100 kcal/mol. The same plot for sample I did not give a straight line. The results obtained above are summarized in Table 2.

Microscopic Observation of the Formation and Growth of Nucleus. Graphite fluoride belongs to optically uniaxial crystals and its optic character is negative. The principal refractive index, ω is 1.543—1.544.[15] In the following observation, since sample was exposed with the light in parallel with the optic axis (or crystallographical c axis) of $(CF)_n$, it apparently looks optically isotropic. Therefore, it looks always dark in the observation between crossed nicols. Figure 9 shows the photomicrographs of the sample before decomposition. The bright lines in Fig. 9B showed double refraction and were extinguished in the rotation of the sample by 90°. A bright line showing double refraction corresponds to the black line in Fig. 9A, and is regarded as grain boundary in $(CF)_n$ crystal.

The sample was heated up to 400 °C in a vacuum with a heating rate of 10 °C/min, and it was then quenched to room temperature. Photomicrographs of the sample after these treatments are shown in Fig. 10. In the case of observation with transmitted light, the black lines in Fig. 10A were widened, and light lines in Fig. 10B were darkened in the observation between crossed nicols. These results suggest that the decom-

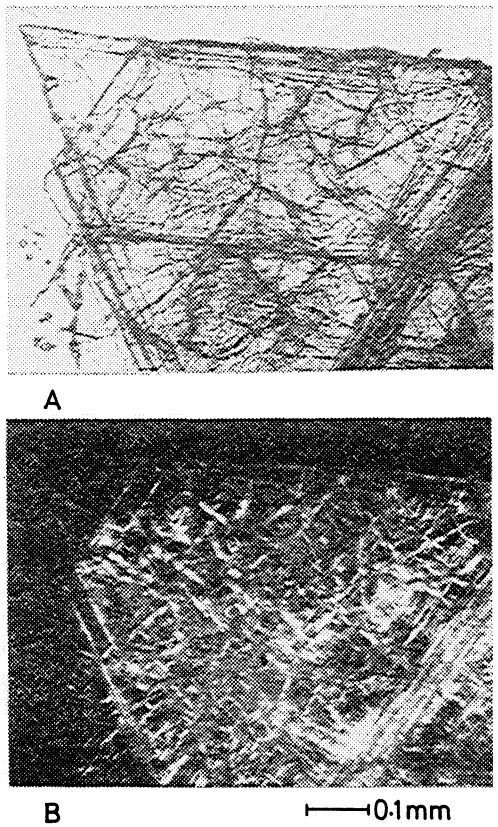

Fig. 9. Photomicrographs of graphite fluoride thin flake.
A: Transmission, B: reflection between crossed nicols.

position nucleus of carbon is formed on the grain boundary.

Figure 11 shows the shape of the nucleus. The main part of the photomicrograph is sketched; the solid line shows the outline of a nucleus, and the broken line shows a grain boudary. Nuclei spread long along the grain boundary, and is anisotropic in shape. Therefore, a nucleus should be formed at a point on a grain boundary and then grow along the grain boundary. The growth of the nucleus is not isotropic, that is, fast along the grain boundary and slow in other directions. Figure 12 shows a scanning electron micrograph and changes in composition of carbon

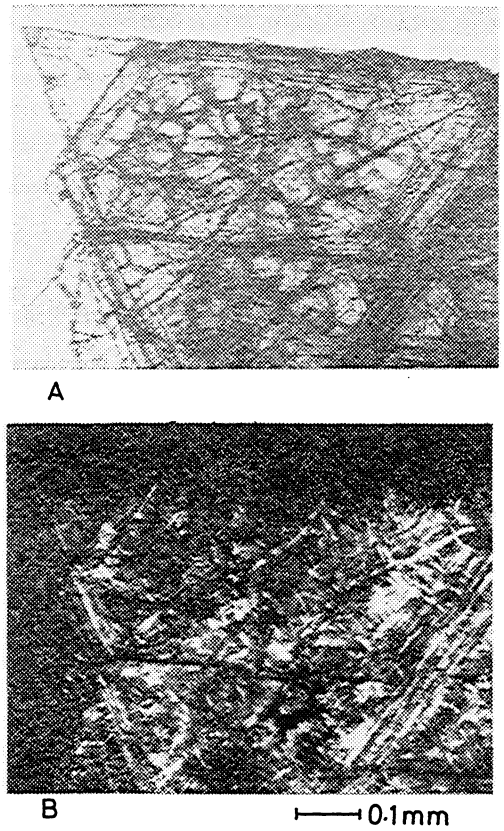

Fig. 10. Photomicrographs of partially decomposed graphite fluoride flake.
A: Transmission, B: reflection between crossed nicols.

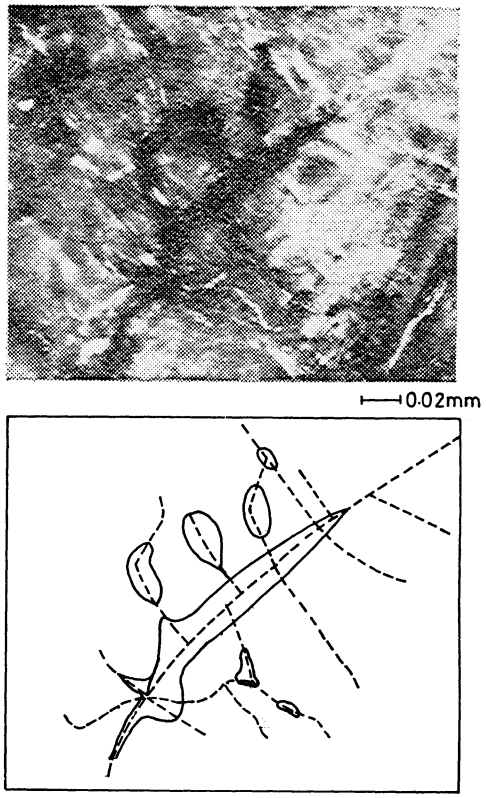

Fig. 11. Photomicrograph of graphite fluoride showing the shape of nuclei (reflection between crossed nicols). Broken line: grain boundary, solid line: nucleus of carbon.

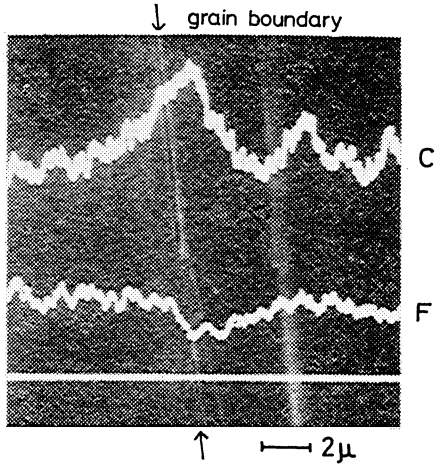

Fig. 12. Scanning electron micrograph of the grain boundary and elemental analysis by X-ray micro-analyzer.

and fluorine atoms determined by means of the X-ray microanalysis. The straight line shows the place where the analysis is done. Two curves above the straight line show the distribution of carbon and fluorine atoms. Fluorine concentration near the grain boundary is low and carbon concentration is high as compared with other parts. No such a change was observed for the original graphite fluoride.

It should be due to the strain energy[15] that the decomposition begins at a point on the grain boundary. This region is energetically activated. The nucleation takes place at the point to which extremely high stress is applied. When the layer plane of $(CF)_n$ is decomposed to that of graphite, the C–C bond length decreases from 1.54 to 1.42 Å, and the plane shrinks.[2] Therefore, the stress applied to the point where the decomposition occurs is relaxed. Next the stress remains in the vicinity along the grain boundary, and then the vicinity will decompose in turn. Thus the nucleus grows along the grain boundary. Because of the relaxation of the stress which expands the layer spacing, the crystallinity of $(CF)_n$ is improved as described in the preceding paper.[3]

Kinetics of Thermal Decomposition of $(CF)_n$. The rate of thermal decomposition of highly oriented $(CF)_n$ is expressed by Eq. 4 with $n=2$. In this equation, it is assumed that the volume $V(t)$ of the nucleus at time t is given by:

$$V(t) = \sigma(k_1 t)^2 \qquad (6)$$

This equation also involves the assumption that the growth of the nucleus is isotropic. When the nucleus grows anisotropically, the volume should not be given by this equation. Figure 13 shows a model of the nucleus shape in $(CF)_n$. A nucleus formed at A at time 0 grows at a rate of k_a along the grain boundary and at a rate of k_b in other directions, where $k_a > k_b$. At time y ($y<t$), the growth of the nucleus reaches to B. At time t, the front of the nucleus spreads by $k_b(t-y)$ from B and by $k_b \cdot t$ from A in other directions than grain boundary. Therefore, the shape of the nucleus

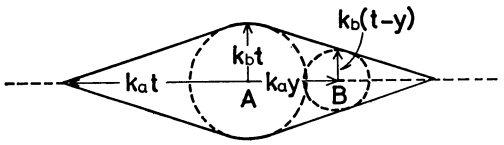

Fig. 13. Schematic model of a nucleus at time t, which was formed at $t=0$.
Broken line: grain boundary.

at time t is rhomb-like as given by the solid line in Fig. 13. The volume of the nucleus having this shape is given by:

$$V(t) = 2\sigma k_a k_b t^2, \qquad (k_a \gg k_b). \tag{7}$$

Then Eq. 4 can be rewritten as[10]

$$-\ln(1-\alpha) = \frac{2\sigma N_0 k_a k_b}{V_0} \cdot t^2. \tag{8}$$

The apparent rate constant, k_1 in Eq. 4 is given by:

$$k_1 = \sqrt{k_a k_b} = A\{\exp(E_{aa}+E_{ab})/2RT\}, \tag{9}$$

where E_{aa} and E_{ab} are the value of activation energy involved in k_a and k_b, respectively. The apparent activation energy according to Eq. 4 is about 50 kcal/mol, that is,

$$E_{aa}/2 + E_{aa}/2 \simeq 50 \text{ (kcal/mol)}. \tag{10}$$

The degree of the nuclei overlapping on the grain boundary becomes larger as the decomposition proceeds because the nucleus forming sites are distributed on the grain boundary. In Avrami-Erofeyev's equation, the overlapping of nuclei has been taken into account.[10] However, Eq. 7 is not applicable if nuclei overlap only on the grain boundary. The number of nucleus forming sites, N_0 of the sample II is greater than that of sample I. The shape of a nucleus of the sample with a large number of nucleus forming sites is shown in Fig. 14. The nuclei overlapping on the grain boundary is negligible in an earlier part of the decomposition as shown in Fig. 14A. On the other hand, it becomes nonnegligible in the later part of the decomposition as shown in Fig. 14B. If the length L of the grain boundary is sufficiently large, the nucleus shown in Fig. 14B is given by:

$$V(t) = 2L\sigma k_b t. \tag{11}$$

Then the rate equation can be written as:

$$-\ln(1-\alpha) = \frac{2L\sigma N_0 k_b}{V_0} \cdot t. \tag{12}$$

This equation has the same form as Eq. 5 and has been applied to the decomposition of sample II (decomposed above 30%) and sample III (decomposed above several percent). The activation energy according to this equation has been obtained to be about 100 kcal/mol, which means $E_{ab} \simeq 100$ kcal/mol. Substituting this value into Eq. 10, a value of almost 0 kcal/mol is obtained as the activation energy for the growth of the nucleus along the grain boundary, that is, $E_{aa} \simeq 0$ kcal/mol.

Characteristics of thermal decomposition of $(CF)_n$. Graphite fluoride, $(CF)_n$ can be regarded as a two-dimensional sheet-like ploymer, and carbon atoms are bonded to fluorine atoms covalently. Chain polymers are generally depolymerized by heat treatment, and

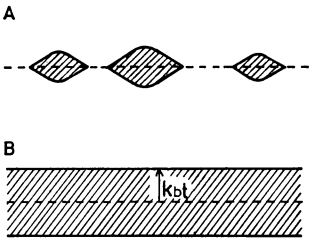

Fig. 14. Schematic illustration of nucleus when the sample has a large number of nucleus forming sites, N_0.
A: Overlapping of nuclei along grain boundary can be neglected, B: grain boundary has perfectly nucleated.

release their corresponding monomer. It seems strange that the decomposition reaction of $(CF)_n$ is heterogeneous as known about magnesite, barium azide, and other ionic crystals.

"Cage effect" is one of the most important phenomena which take place during γ-ray irradiation on some polymers.[16] This effect is essentially the trapping of radicals or molecules formed by the rupture of the polymer chain in polymer molecules. Then these are to recombine with the polymer radicals resulting from the rupture. This is also the case for thermal decomposition of $(CF)_n$. Carbon atoms in the layer is hardly released because they are bonded to neighboring three carbon atoms. Even if one C–C bond is ruptured, the remaining two bonds hold the carbon atom. The probability of recombination should increase, and the decomposition takes place preferentially at the interface between the nucleus and reactant. In fact, decomposition is also initiated on the surface of the crystal and proceeds to the inner part when γ-ray is irradiated on $(CF)_n$.[13] In the case of $(CF)_n$, this effect should be called as "chain effect" rather than "cage effect."

It is due to the strong stress to the grain boundary that thermal decomposition of $(CF)_n$ is initiated at grain boundary. The strain in grain boundary also leads to the decomposition at such a low temperature as 400 °C and zero activation energy E_{aa}. The strain energy remains in the vicinity, and the nucleus grows along the grain boundary.

The actual decomposition mechanism might be more complicated because the grain boundary does not have regular form, and therefore, the shape of the nucleus must change with that of the grain boundary. Consequently, it is not enough to consider only the simple model shown in Fig. 13 for the explanation of the whole reaction. Both Eqs. 8 and 12 could not be applied in the region $\alpha=40$—100% for sample I.

Conclusion

Thermal decomposition of $(CF)_n$ is initiated at a point on a grain boundary or at CF_2 or CF_3 group on the surface of a particle. The nucleus of carbon formed spreads two-dimensionally but anisotropically; the rate of the nucleus growth is larger along the grain boundary than in other directions. As a result,

the shape of nucleus varies with the degree of nucleus overlapping along grain boundary, and the reaction is expressed by either of two different equations. The apparent rate of thermal decomposition is determined by the number of nucleus forming sites in $(CF)_n$ sample.

References

1) N. Watanabe and A. Shibuya, *Kogyo Kagaku Zasshi*, **71**, 963 (1968).
2) M. Takashima and N. Watanabe, *Nippon Kagaku Kaishi*, **1975**, 432.
3) N. Watanabe, S. Koyama, and H. Imoto, *Bull. Chem. Soc. Jpn.*, **53**, 2731 (1980).
4) P. Kamarchik Jr., and J. L. Margrave, *J. Therm. Anal.*, **11**, 259 (1977).
5) Y. Kita, N. Watanabe, and Y. Fujii, *J. Am. Chem. Soc.*, **101**, 3832 (1979).
6) N. Watanabe and H. Takenaka, 5th European Symposium on Fluorine Chemistry, Aviemore Scotland, 16—20th Sept. (1974).
7) M. Takashima and N. Watanabe, *Nippon Kagaku Kaishi*, **1976**, 1222.
8) H. Hashimoto, *Kogyo Kagaku Zasshi*, **63**, 471 (1960).
9) F. E. Harvey, *Trans. Faraday Soc.*, **29**, 653 (1933).
10) Heterogeneous reactions which are seen in decomposition of solids begin at definite localized spot where the activation energy is least. These spots are called nuleus forming sites. A nucleus forming site becomes a small nucleus of reaction product by initial reaction. Once the nucleation takes place, the nucleus spreads 1-, 2-, or 3-dimensionally since the reactant becomes active at the interface with the product. The detailed description about the mechanism of the nucleation and the growth of the nucleus is given in: P. W. M. Jacobs and F. C. Tompkins, "Classification and Theory of Solid Reactions," in "Chemistry of Solid State," ed by W. E. Garner, Butterworth (1955), pp. 184—212.
11) In the case of $(CF)_n$, a small particle of carbon formed by initial decomposition can be regarded as a nucleus.
12) M. Avrami, *J. Chem. Phys.*, **8**, 212 (1940).
13) N. Watanabe, S. Koyama, Y. Kita, and M. Iwasaki, *Nippon Kagaku Kaishi*, **1978**, 1618.
14) N. Watanabe and Y. Kita, *Nippon Kagaku Kaishi*, **1975**, 1896.
15) N. Watanabe and H. Takenaka, *Tanso*, **92**, 2 (1978).
16) K. Shinohara and H. Kashiwabara, "Hoshasen to Kobunshi," Maki Shoten (1968), p. 68.